Stem Cell Reports, Volume *14*

Supplemental Information

Overexpression of Nuclear Receptor 5A1 Induces and Maintains an Intermediate State of Conversion between Primed and Naive Pluripotency

Kaori Yamauchi, Tatsuhiko Ikeda, Mihoko Hosokawa, Norio Nakatsuji, Eihachiro Kawase, Shinichiro Chuma, Kouichi Hasegawa, and Hirofumi Suemori

Figure S1

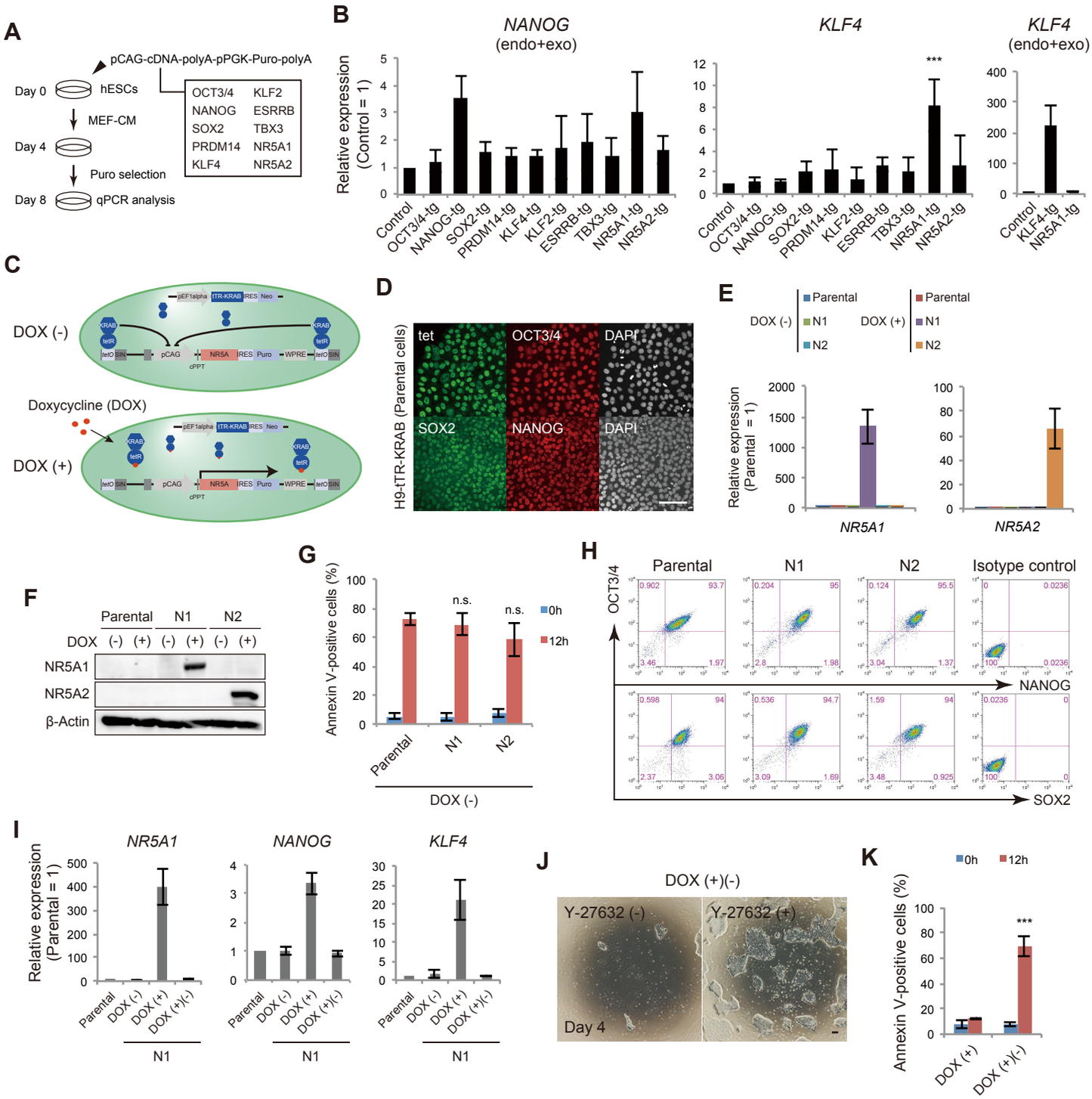
A
pCAG-cDNA-polyA-pPGK-Puro-polyA
Day 0
hESCs
MEF-CM
Day 4
Puro selection
Day 8
qPCR analysis
OCT3/4 KLF2
NANOG ESRRB
SOX2 TBX3
PRDM14 NR5A1
KLF4 NR5A2
B
NANOG (endo+exo)
KLF4
KLF4 (endo+exo)
Relative expression (Control = 1)
***
Control
OCT3/4-tg
NANOG-tg
SOX2-tg
PRDM14-tg
KLF4-tg
KLF2-tg
ESRRB-tg
TBX3-tg
NR5A1-tg
NR5A2-tg
C
DOX (-)
Doxycycline (DOX)
DOX (+)
D
H9-tTR-KRAB (Parental cells)
tet
OCT3/4
DAPI
SOX2
NANOG
DAPI
E
Parental
N1
N2
DOX (-)
DOX (+)
Relative expression (Parental = 1)
NR5A1
NR5A2
F
Parental
N1
N2
DOX (-) (+) (-) (+) (-) (+)
NR5A1
NR5A2
β-Actin
G
Annexin V-positive cells (%)
n.s.
n.s.
0h
12h
Parental
N1
N2
DOX (-)
H
Parental
N1
N2
Isotype control
OCT3/4
NANOG
SOX2
I
NR5A1
NANOG
KLF4
Relative expression (Parental = 1)
Parental
DOX (-)
DOX (+)
DOX (+)(-)
N1
J
DOX (+)(-)
Y-27632 (-)
Y-27632 (+)
Day 4
K
0h
12h
Annexin V-positive cells (%)
***
DOX (+)
DOX (+)(-)

Figure S2

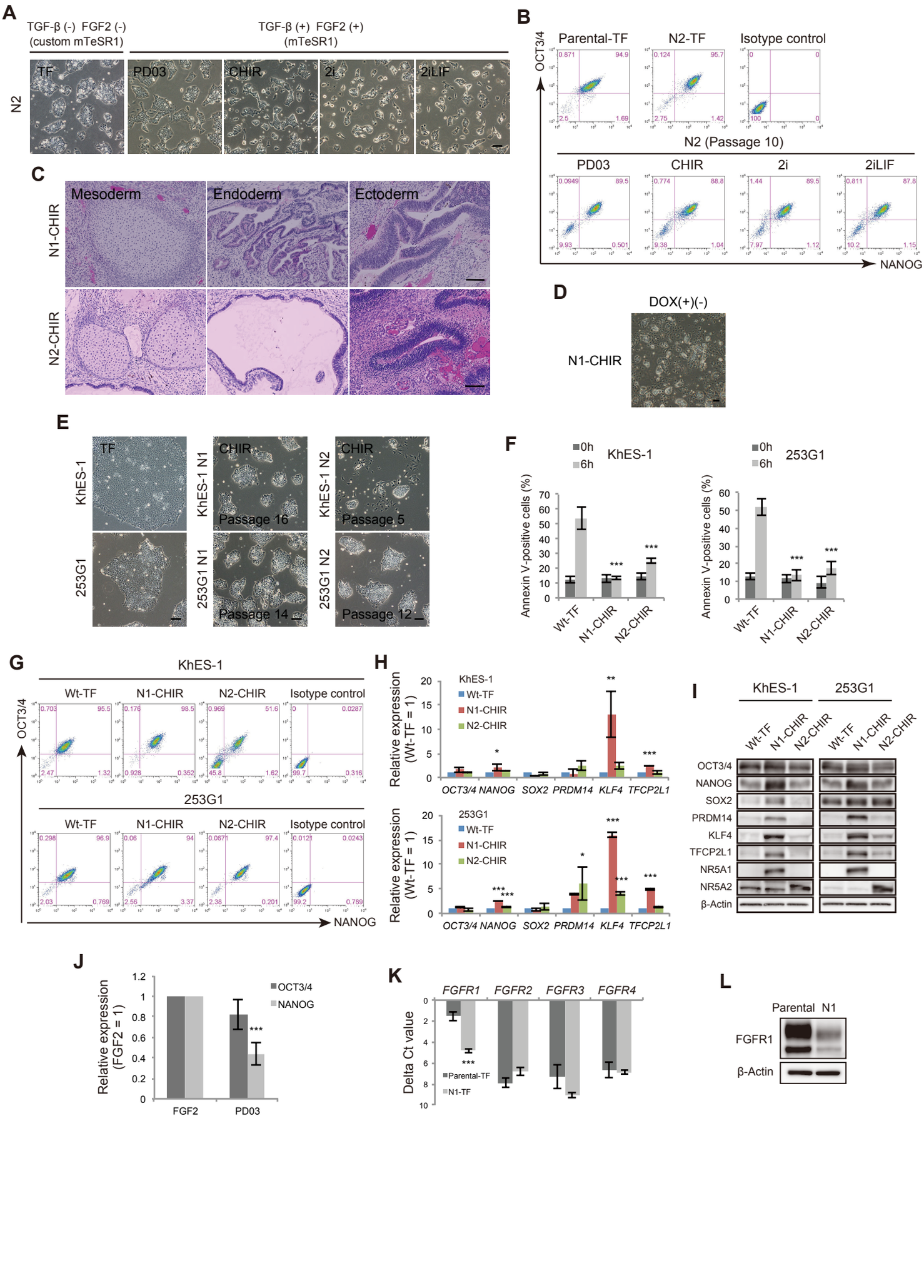
A
TGF-β (-) FGF2 (-)
(custom mTeSR1)
TGF-β (+) FGF2 (+)
(mTeSR1)
N2
TF
PD03
CHIR
2i
2iLIF
B
Parental-TF
N2-TF
Isotype control
OCT3/4
N2 (Passage 10)
PD03
CHIR
2i
2iLIF
NANOG
C
N1-CHIR
N2-CHIR
Mesoderm
Endoderm
Ectoderm
D
DOX(+)(-)
N1-CHIR
E
KhES-1
253G1
TF
KhES-1 N1
253G1 N1
CHIR
Passage 16
Passage 14
KhES-1 N2
253G1 N2
CHIR
Passage 5
Passage 12
F
0h
6h
KhES-1
253G1
Annexin V-positive cells (%)
Wt-TF
N1-CHIR
N2-CHIR
G
KhES-1
Wt-TF
N1-CHIR
N2-CHIR
Isotype control
OCT3/4
253G1
NANOG
H
KhES-1
Wt-TF
N1-CHIR
N2-CHIR
Relative expression
(Wt-TF = 1)
OCT3/4 NANOG SOX2 PRDM14 KLF4 TFCP2L1
253G1
I
KhES-1
253G1
Wt-TF
N1-CHIR
N2-CHIR
OCT3/4
NANOG
SOX2
PRDM14
KLF4
TFCP2L1
NR5A1
NR5A2
β-Actin
J
Relative expression
(FGF2 = 1)
OCT3/4
NANOG
FGF2
PD03
K
FGFR1 FGFR2 FGFR3 FGFR4
Delta Ct value
Parental-TF
N1-TF
L
Parental N1
FGFR1
β-Actin

Figure S3

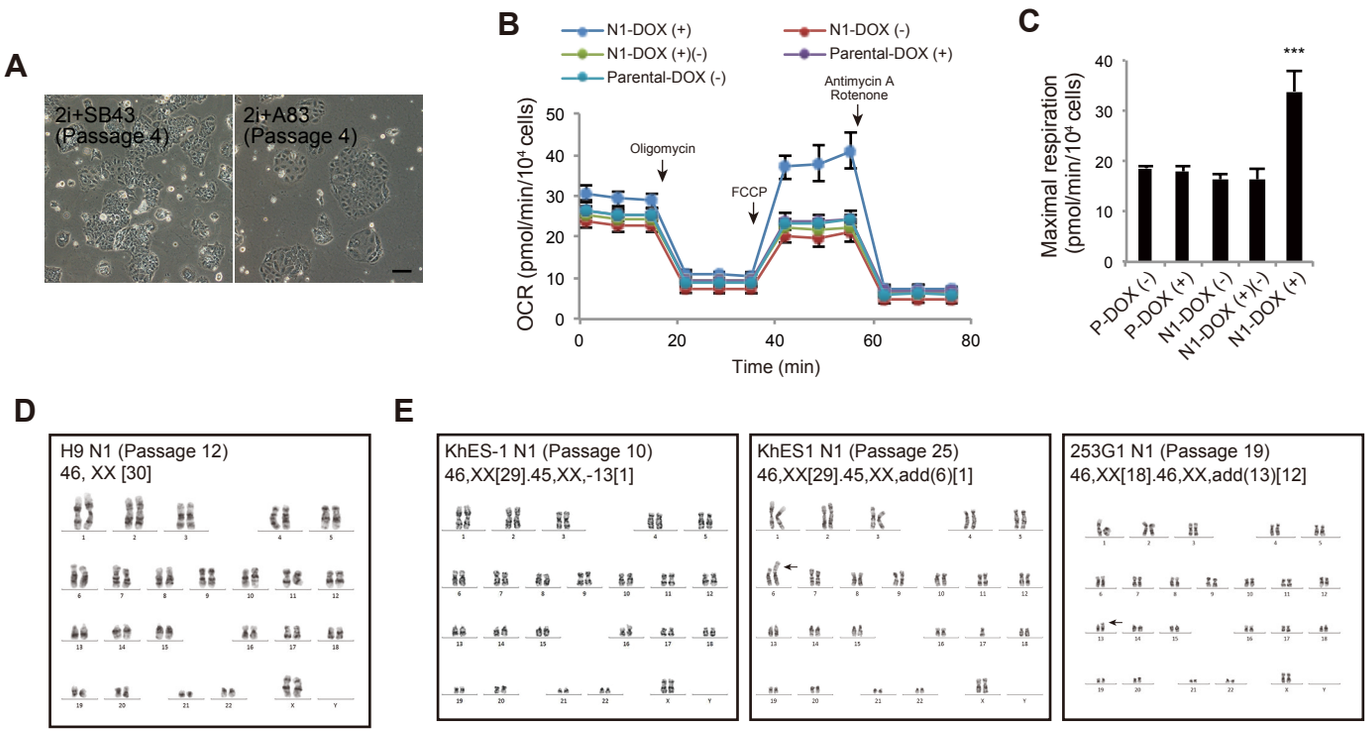
A
2i+SB43
(Passage 4)
2i+A83
(Passage 4)
B
N1-DOX (+)
N1-DOX (-)
N1-DOX (+)(-)
Parental-DOX (+)
Parental-DOX (-)
Antimycin A
Rotenone
Oligomycin
FCCP
OCR (pmol/min/10^4 cells)
Time (min)
C
***
Maximal respiration
(pmol/min/10^4 cells)
P-DOX (-)
P-DOX (+)
N1-DOX (-)
N1-DOX (+)(-)
N1-DOX (+)
D
H9 N1 (Passage 12)
46, XX [30]
E
KhES-1 N1 (Passage 10)
46,XX[29].45,XX,-13[1]
KhES1 N1 (Passage 25)
46,XX[29].45,XX,add(6)[1]
253G1 N1 (Passage 19)
46,XX[18].46,XX,add(13)[12]

Figure S4

A

Upregulated genes in parental-CHIR

Category	Term	Count	PValue
GOTERM_BP_FAT	GO:0030182~neuron differentiation	90	1.70E-29
	GO:0000904~cell morphogenesis involved in differentiation	56	9.79E-21
	GO:0007423~sensory organ development	54	1.41E-20
GOTERM_CC_FAT	GO:0031012~extracellular matrix	60	2.04E-17
	GO:0044421~extracellular region part	109	2.12E-16
	GO:0005578~proteinaceous extracellular matrix	56	3.19E-16
GOTERM_MF_FAT	GO:0043565~sequence-specific DNA binding	86	2.56E-17
	GO:0003700~transcription factor activity	107	2.01E-13
	GO:0030528~transcription regulator activity	142	2.25E-12
KEGG_PATHWAY	hsa05217:Basal cell carcinoma	21	2.18E-13
	hsa04340:Hedgehog signaling pathway	19	4.05E-11
	hsa04310:Wnt signaling pathway	25	1.44E-07

Upregulated genes in N1-CHIR

Category	Term	Count	PValue
GOTERM_BP_FAT	GO:0051240~positive regulation of multicellular organismal process	35	5.38E-08
	GO:0009611~response to wounding	57	8.02E-08
	GO:0006952~defense response	62	2.03E-07
GOTERM_CC_FAT	GO:0005576~extracellular region	175	1.94E-15
	GO:0044421~extracellular region part	100	4.44E-13
	GO:0005615~extracellular space	71	2.67E-09
GOTERM_MF_FAT	GO:0005125~cytokine activity	27	5.72E-06
	GO:0008083~growth factor activity	24	6.19E-06
	GO:0030246~carbohydrate binding	35	2.49E-04
KEGG_PATHWAY	hsa04060:Cytokine-cytokine receptor interaction	33	1.20.E-05
	hsa00980:Metabolism of xenobiotics by cytochrome P450	11	1.38.E-03
	hsa05200:Pathways in cancer	30	6.54.E-03

Downregulated genes in parental-CHIR

Category	Term	Count	PValue
GOTERM_BP_FAT	GO:0009611~response to wounding	66	4.03E-07
	GO:0042127~regulation of cell proliferation	85	3.07E-06
	GO:0050865~regulation of cell activation	29	7.45E-06
GOTERM_CC_FAT	GO:0044459~plasma membrane part	241	2.36E-16
	GO:0005887~integral to plasma membrane	140	1.69E-11
	GO:0031226~intrinsic to plasma membrane	140	8.47E-11
GOTERM_MF_FAT	GO:0046870~cadmium ion binding	8	5.11E-07
	GO:0005507~copper ion binding	15	1.27E-04
	GO:0008289~lipid binding	51	1.62E-04
KEGG_PATHWAY	hsa04060:Cytokine-cytokine receptor interaction	35	3.95.E-04
	hsa04514:Cell adhesion molecules (CAMs)	21	9.64.E-04
	hsa04080:Neuroactive ligand-receptor interaction	33	1.12.E-03

Downregulated genes in N1-CHIR

Category	Term	Count	PValue
GOTERM_BP_FAT	GO:0022610~biological adhesion	56	2.65E-08
	GO:0007155~cell adhesion	55	6.45E-08
	GO:0007507~heart development	24	2.57E-06
GOTERM_CC_FAT	GO:0044459~plasma membrane part	131	2.60E-07
	GO:0005578~proteinaceous extracellular matrix	33	9.72E-07
	GO:0031012~extracellular matrix	34	1.80E-06
GOTERM_MF_FAT	GO:0004714~transmembrane receptor protein tyrosine kinase activity	12	3.22E-05
	GO:0005509~calcium ion binding	55	4.94E-04
	GO:0019838~growth factor binding	13	5.08E-04
KEGG_PATHWAY	hsa04510:Focal adhesion	17	1.37.E-03
	hsa04514:Cell adhesion molecules (CAMs)	12	5.44.E-03
	hsa04512:ECM-receptor interaction	8	2.48.E-02

B

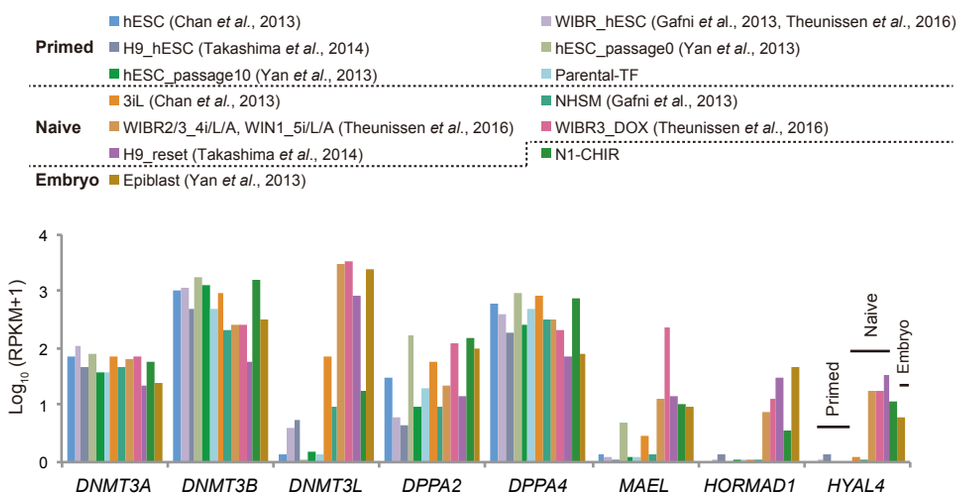

C

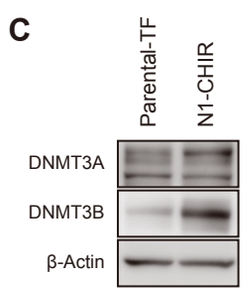

D

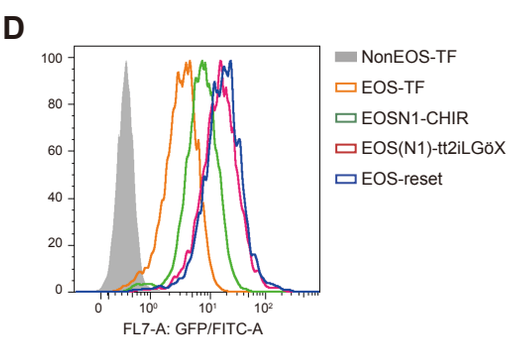

E

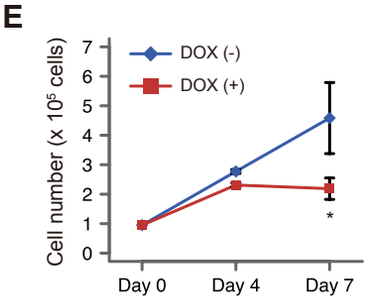

F

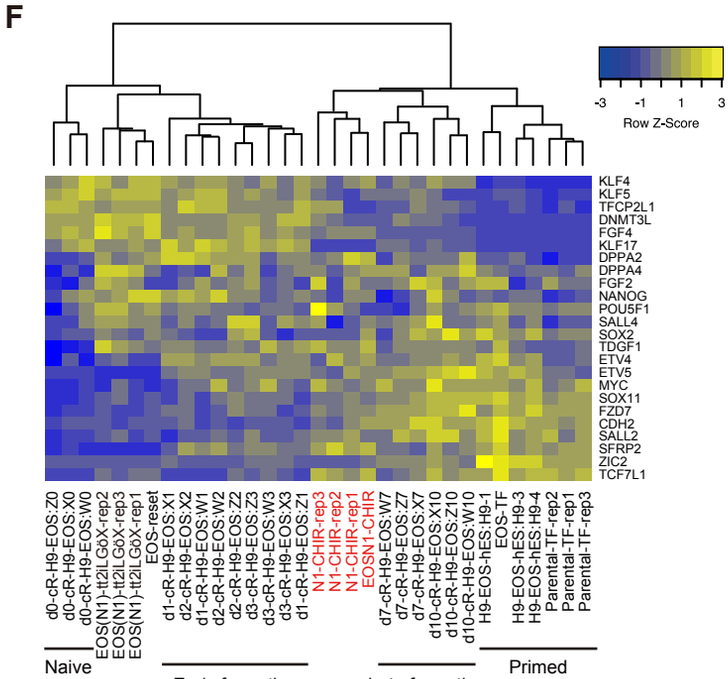

Figure S5

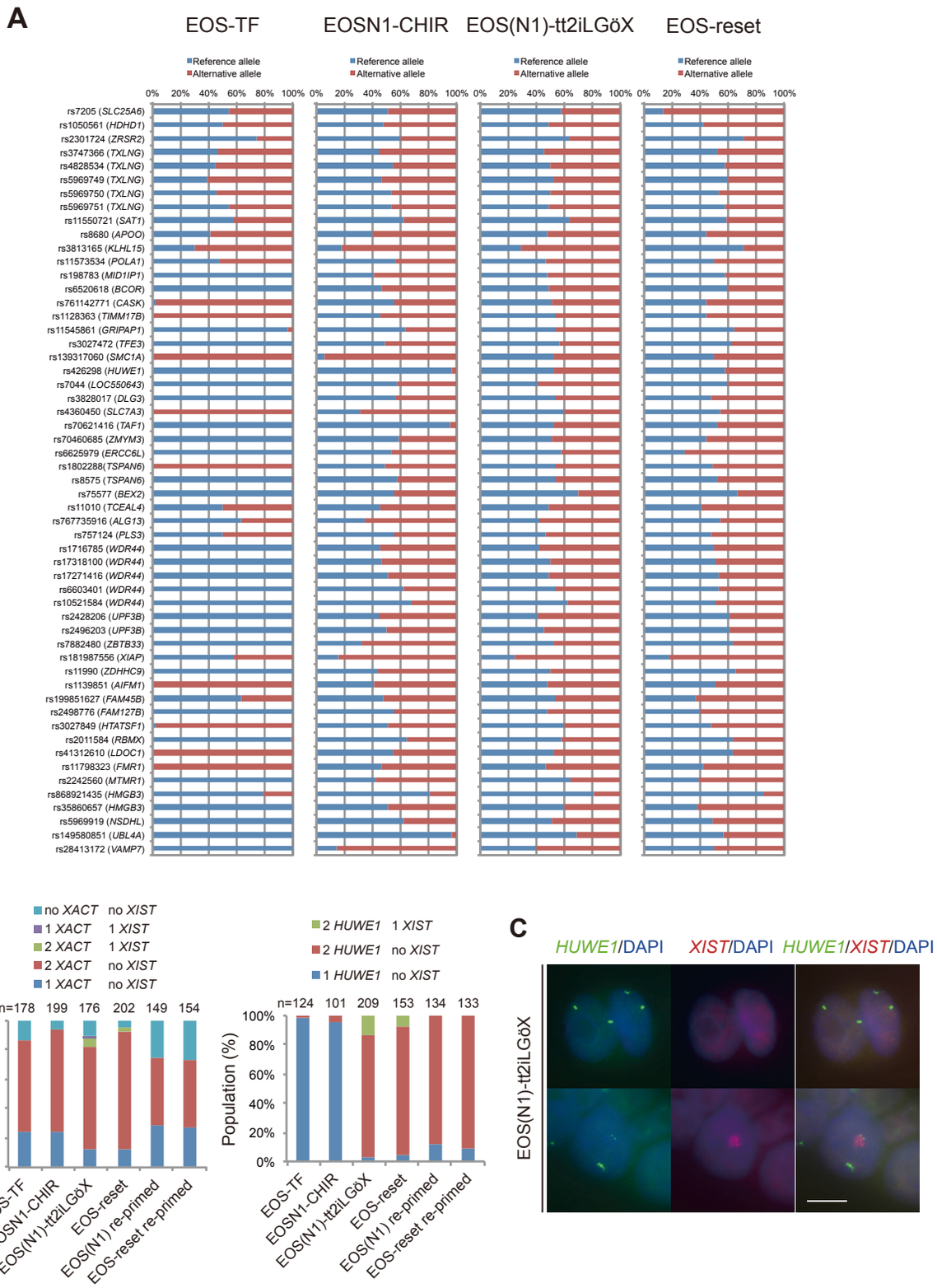
A
EOS-TF
EOSN1-CHIR
EOS(N1)-tt2iLGöX
EOS-reset
Reference allele
Alternative allele
0% 20% 40% 60% 80% 100%
rs7205 (SLC25A6)
rs1050561 (HDHD1)
rs2301724 (ZRSR2)
rs3747366 (TXLNG)
rs4828534 (TXLNG)
rs5969749 (TXLNG)
rs5969750 (TXLNG)
rs5969751 (TXLNG)
rs11550721 (SAT1)
rs8680 (APOO)
rs3813165 (KLHL15)
rs11573534 (POLA1)
rs198783 (MID1IP1)
rs6520618 (BCOR)
rs761142771 (CASK)
rs1128363 (TIMM17B)
rs11545861 (GRIPAP1)
rs3027472 (TFE3)
rs139317060 (SMC1A)
rs426298 (HUWE1)
rs7044 (LOC550643)
rs3828017 (DLG3)
rs4360450 (SLC7A3)
rs70621416 (TAF1)
rs70460685 (ZMYM3)
rs6625979 (ERCC6L)
rs1802288(TSPAN6)
rs8575 (TSPAN6)
rs75577 (BEX2)
rs11010 (TCEAL4)
rs767735916 (ALG13)
rs757124 (PLS3)
rs1716785 (WDR44)
rs17318100 (WDR44)
rs17271416 (WDR44)
rs6603401 (WDR44)
rs10521584 (WDR44)
rs2428206 (UPF3B)
rs2496203 (UPF3B)
rs7882480 (ZBTB33)
rs181987556 (XIAP)
rs11990 (ZDHHC9)
rs1139851 (AIFM1)
rs199851627 (FAM45B)
rs2498776 (FAM127B)
rs3027849 (HTATSF1)
rs2011584 (RBMX)
rs41312610 (LDOC1)
rs11798323 (FMR1)
rs2242560 (MTMR1)
rs868921435 (HMGB3)
rs35860657 (HMGB3)
rs5969919 (NSDHL)
rs149580851 (UBL4A)
rs28413172 (VAMP7)
B
no XACT no XIST
1 XACT 1 XIST
2 XACT 1 XIST
2 XACT no XIST
1 XACT no XIST
n=178 199 176 202 149 154
Population (%)
EOS-TF
EOSN1-CHIR
EOS(N1)-tt2iLGöX
EOS-reset
EOS(N1) re-primed
EOS-reset re-primed
2 HUWE1 1 XIST
2 HUWE1 no XIST
1 HUWE1 no XIST
n=124 101 209 153 134 133
C
HUWE1/DAPI
XIST/DAPI
HUWE1/XIST/DAPI
EOS(N1)-tt2iLGöX

Figure S6

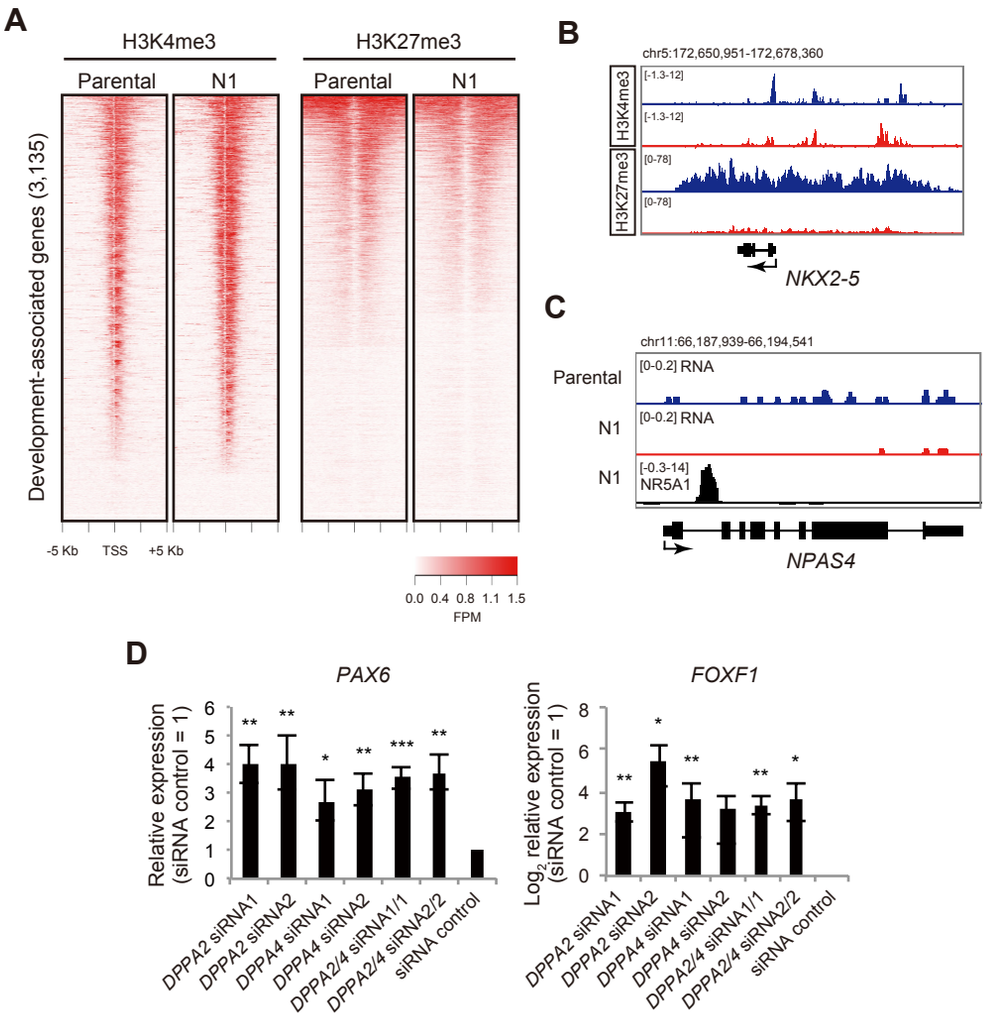
A
H3K4me3
H3K27me3
Parental
N1
Parental
N1
Development-associated genes (3,135)
-5 Kb
TSS
+5 Kb
0.0 0.4 0.8 1.1 1.5
FPM
B
chr5:172,650,951-172,678,360
H3K4me3
[-1.3-12]
[-1.3-12]
H3K27me3
[0-78]
[0-78]
NKX2-5
C
chr11:66,187,939-66,194,541
Parental
[0-0.2] RNA
N1
[0-0.2] RNA
N1
[-0.3-14]
NR5A1
NPAS4
D
PAX6
Relative expression (siRNA control = 1)
FOXF1
Log2 relative expression (siRNA control = 1)
DPPA2 siRNA1
DPPA2 siRNA2
DPPA4 siRNA1
DPPA4 siRNA2
DPPA2/4 siRNA1/1
DPPA2/4 siRNA2/2
siRNA control

Supplemental Figure Legends

Figure S1. Analysis of NR5A-induced cells under the TF condition (related to Figure 1).

(A) Scheme of the gene expression system used to screen the indicated transcription factors.

(B) Expression of *NANOG* and *KLF4* in control cells and transfectants. Data were analyzed by the comparative ΔCt method. Expression in control cells transfected with empty vector was set to 1. Endo and exo represent endogenous and exogenous expression, respectively. ***$p < 0.001$ (Dunnett's test).

(C) Scheme of the doxycycline (DOX)-inducible gene expression system used in this study. In the absence of DOX [DOX (–)], a fusion protein of tetracycline (tet) repressor (tTR) and a Krüppel-associated box (KRAB) domain binds to tet operator (*tetO*) sequences and suppresses expression of NR5A. Addition of DOX [DOX (+)] blocks the binding of tTR-KRAB to *tetO*, resulting in transgene expression.

(D) Immunocytochemical staining of tet and pluripotency markers, such as OCT3/4, NANOG, and SOX2, in a parental clone expressing tTR-KRAB.

(E) NR5A expression analyzed by qPCR. Data were analyzed by the comparative ΔCt method. Parental cell expression was set to 1. NR5A1- and NR5A2-expressing cells are referred to as N1 and N2 cells, respectively.

(F) NR5A expression analyzed by western blotting. β-Actin was used as a loading control.

(G) Percentages of annexin V-positive cells before (0 h) and 12 h after single cell dissociation. Parental, N1, and N2 cells were cultured in the absence of DOX. The numbers of positive cells were analyzed by flow cytometry. Statistical significance vs. parental cells at 0 or 12 h (Dunnett's test). n.s., not significant.

(H) Flow cytometric analysis of pluripotency markers in parental, N1, and N2 cells.

(I) Expression of the indicated genes analyzed by qPCR. Data were analyzed by the comparative ΔCt method. Parental cell expression was set to 1. N1-DOX (+)(–) represents cells after withdrawal of DOX.

(J) Representative images of the NR5A1 transfectant after DOX withdrawal. Cells were seeded in the absence or presence of Y-27632 (+).

(K) Percentages of annexin V-positive cells before (0 h) and 12 h after single cell dissociation. ***$p < 0.001$ (Student's *t*-test).

Data are represented as mean ± SD (B, E, G, and I) or SEM (G and K) of three biological replicates. Scale bars = 100 μm.

Figure S2. NR5A-induced cells maintain pluripotency in the presence of a GSK3 inhibitor (related to Figure 2).

(A) Representative images of N2 cells cultured under TF or 2i conditions.

(B) Flow cytometric analysis of pluripotency markers in parental and N2 cells under each condition.

(C) Teratoma formation of N1 and N2 cells after passages 10.

(D) Representative image of N1 cells after withdrawal of DOX under the CHIR condition.

(E) Representative images of control cells and NR5A transfectants derived from KhES-1 and 253G1 cells. The cells were cultured under TF or CHIR conditions.

(F) Percentages of annexin V-positive cells among control cells and NR5A transfectants derived from KhES-1 and 253G1 cells 6 h after single cell dissociation. ***$p < 0.001$ vs. wild type cells (Dunnett's test).

(G) Flow cytometric analysis of pluripotency markers in control cells and NR5A transfectants derived from KhES-1 and 253G1 under each condition.

(H and I) Expression of transcripts and proteins associated with the naive pluripotent state in control cells and NR5A transfectants derived from KhES-1 and 253G1. Data were analyzed by the comparative ΔCt method. Expression in unmodified hPSCs cultured in the TF condition (Wt) was set to 1. β-Actin was used as a loading control.

(J) Expression of *POU5F1* and *NANOG* in parental cells 24 h after PD03 treatment. Data were analyzed by the comparative ΔCt method. Expression in the FGF condition was set to 1.

(K) Expression of *FGFRs* in parental and NR5A1-induced cells cultured under the TF condition. Data analyzed by qPCR are shown as ΔCt values.

(L) Western blotting of FGFR1 in parental and NR5A1-induced cells cultured under the TF condition. β-Actin was used as a loading control.

Scale bars = 100 μm. Data are represented as mean ± SD (G–K) or SEM (F) of three biological replicates. ***$p < 0.001$ (Student's *t*-test; J, K).

Figure S3. Characterizations of NR5A-induced cells cultured in the presence of a GSK3 inhibitor (related to Figure 2)

(A) Representative images of NR5A1-induced cells cultured with inhibitors of TGF-β/activin/nodal signaling.

(B and C) Oxygen consumption rate (OCR) assay under mitochondrial stress. N1-DOX (+) and N1-DOX (–) cells were cultured under CHIR or TF conditions. N1-DOX (+)(–) represents cells after withdrawal of DOX. Data are represented as mean ± SD of five biological replicates ***$p < 0.001$ vs. P-DOX (–) cells (Dunnett's test).

(D and E) Karyotype analysis of H9 N1 (M), KhES-1 N1 (N, left and middle panels), and 253G1 N1 (N, right panel) cells cultured with CHIR. Thirty metaphases from cells maintained by single cell passaging for the indicated passage numbers were analyzed.

Scale bars = 100 μm.

Figure S4. Global analysis of gene expression under NR5A1 regulation (related to Figure 3).

(A) Gene Ontology (GO) analysis of up- and downregulated genes in CHIR-treated parental and NR5A1-induced cells.

(B) RNA-seq analysis of the indicated genes. Data are shown as the $\log_{10}$ (RPKM+1). RPKM, reads per kilobase of exon per million mapped reads.

(C) DNMT3A and DNMT3B expression analyzed by western blotting. β-Actin was used as a loading control.

(D) Flow cytometric analysis of GFP expression under each condition.

(E) Proliferation analysis of EOS-N1 cells in the absence or presence of DOX under the tt2iLGöX condition. Data are represented as mean ± SD of three biological replicates. *$p < 0.005$ (Student's *t*-test).

(F) Heat map of genes selected from RNA-seq data of this study and previously published study relating to formative transition (Rostovskaya et al., 2019).

Figure S5. Conversion of NR5A1-induced cells to the full naive pluripotent state under the tt2iLGöX condition (related to Figure 4).

(A) Single nucleotide polymorphism (SNP)-based allelic expression patterns of the two X chromosomes. The allelic expression patterns of representative genes analyzed in RNA-seq data are shown with their reference SNP IDs (rs).

(B) Percentages of cells bearing different X chromosome statuses. Data were analyzed by RNA- fluorescence in situ hybridization (FISH) of *XACT*, *HUWE1*, and *XIST* in each condition.

(C) Representative RNA-FISH images of *HUWE1* and *XIST* in EOS(N1)-tt2iLGöX cells. Scale bars = 10 μm.

Figure S6. Chromatin immunoprecipitation sequencing (ChIP-seq) analysis of NR5A1 in CHIR-treated NR5A1-induced cells (related to Figure 5).

(A) Heat maps based on H3K4me3 and H3K27me3 signal enrichment around the transcriptional start sites (TSSs) of development-associated genes (Theunissen et al., 2014).

(B) NR5A1 signal distribution on the *NKX2-5* gene in NR5A1-induced cells. Data analyzed by RNA-seq are also shown.

(C) NR5A1 signal distribution on the *NPAS4* gene in NR5A1-induced cells. Data analyzed by RNA-seq are also shown.

(D) Depletion of *DPPA2* and *DPPA4* in NR5A1-induced cells by siRNA. Data were analyzed by the comparative ΔCt method. Expression in cells treated with control siRNA were set to 1. *$p < 0.05$, **$p < 0.01$, ***$p < 0.001$ (Student's *t*-test).

Supplemental Tables

Table S1. Primer sequences used in this study (related to the Experimental Procedures)

Gene	Forward	Reverse	Use
NR5A1	atttaaatatggactacaaggacgatgac	atttaaattcaagtctgcttggcttgca	Cloning
NR5A1	gaagcttgactattcgtacgacga	ggatcctcaagtctgcttggctt	3×FLAG
NR5A2	atttaaatctaagaatgtcttctaattcag	atttaaatttaaaccttatcgtcgtcatc	Cloning
NR5A2	caaggttaccaaacatatggccactttccta	taggaaagtggccatatgtttggtaaccttg	Mutagenesis
GAPDH	gaaggtgaaggtcggagtc	gaagatggtgatgggatttc	RT-qPCR
ACTB	catgtacgttgctatccaggc	ctccttaatgtcacgcacga	RT-qPCR
HPRT	tggtcaggcagtataatccaaaga	tcaaatccaacaaagtctggctta	RT-qPCR
RPL37A	ccaaacgtaccaagaaagtcgg	gcgtgctggctgatttcaa	RT-qPCR
OCT3/4	gaaggagaagctggagcaaa	catcggcctgtgtatatccc	RT-qPCR
NANOG	ctgctgagatgcctcacacg	tgcctttgggactggtgga	RT-qPCR
SOX2	ggcagctacagcatgatgcaggacc	tggtcatggagttgtactgcagg	RT-qPCR
PRDM14	tgagccttcaggtcacagag	atttcctatcgcccttgtcc	RT-qPCR
KLF4	gggcccaattacccatcctt	ctttggcttgggctcctctg	RT-qPCR
TFCP2L1	gctcttcaacgccatcaaa	caggggcactcgattctg	RT-qPCR
DPPA2	accctgaacaacggcaag	ttgcgtttcctcgaacatc	RT-qPCR
DPPA4	cctcctgggcgagaattt	gaccacacaccacctgacac	RT-qPCR
DPPA3	gaccaacaaacaaggagcctaag	agaaggatccatccattagaca	RT-qPCR
ZFP42	cagaacagaagaggccttcac	tctgagtaagctgtcttcagcaa	RT-qPCR
NR5A1	gcaggtgcatggtcttcaa	agttctgcagcagcgtcat	RT-qPCR
NR5A2	ccgacaagtggtacatggaa	tccggcttgtgatgctatta	RT-qPCR
FGFR1	actccggcctctatgcttg	aggaggggagagcatctga	RT-qPCR
FGFR2	cctgccaaaacagcaagc	aagacccctatgcagtaaatgg	RT-qPCR
FGFR3	tcctcgggagatgacgaa	cagcagcttcttgtccatcc	RT-qPCR
FGFR4	gaggggccgcctagagatt	caggacgatcatggagcct	RT-qPCR
FGF4	gcaagggcaagctctatgg	tgtaggactcgtaggcgttgt	RT-qPCR
PAX6	gcttcaccatggcaaataacc	ggcagcatgcaggagtatga	RT-qPCR
FOXF1	acagcggcgcctcttatatc	ctcctttcggtcacacatgc	RT-qPCR

Genes	Forward	Reverse		References
NANOG	tggttaggttggttttaaatttttg	aacccacccttataaattctcaatta	Bisulfite-PCR	(Takahashi et al., 2007)
PEG10	ggtgtaatttatataaggtttatagtttg	aacaaaaaaaataaaatcccacac	Bisulfite-PCR	(Kim et al., 2007)
SNURF/ SNRPN	taggttgtttttgagagaagttat	aaaaaaactaaaacccctacactac	Bisulfite-PCR	(Kim et al., 2007)

RT-qPCR, quantitative reverse transcription polymerase chain reaction.

Table S2. Antibodies used in this study

Antibody	Company	Catalog Number	Dilution
OCT3/4 (C-10)	Santa Cruz Biotechnology	sc-5279	1:300 for immunocytochemistry 1:1000 for western blotting
NANOG	Cell Signaling Technology	4903	1:300 for immunocytochemistry 1:1000 for western blotting
KLF4 (H-180)	Santa Cruz Biotechnology	sc-20691	1:300 for immunocytochemistry 1:1000 for western blotting
SOX2	R&D Systems	245610	1:500 for immunocytochemistry 1:1000 for western blotting
PRDM14	Abgent	AP1214a	1:500 for western blotting
Tet Repressor	Molecular Biotechnology	TET01	1:200 for immunocytochemistry
DDDDK-tag (FLA-1)	MBL	M185-3L	1:5000 for immunocytochemistry 1:10000 for western blotting ChIP
NR5A1	Perseus Proteomics	PP-N1665-00	1:1000 for western blotting
NR5A2	Perseus Proteomics	PP-H2325-00	1:1000 for western blotting
TFCP2L1	R&D Systems	AF5726	1:1000 for western blotting
β-Actin	Sigma	AC-15	1:5000 for western blotting
Phosho-MEK1/2 (Ser217/221)	Cell Signaling Technology	9121	1:1000 for western blotting
MEK1/2 (L38C12)	Cell Signaling Technology	4694	1:1000 for western blotting
Phospho-p44/42 MAPK (Erk1/2)	Cell Signaling Technology	9106	1:1000 for western blotting

(Thr202/Tyr204) (E10)			
p44/42 MAPK (Erk1/2)	Cell Signaling Technology	9102	1:1000 for western blotting
FGFR1	Abcam	Ab76464	1:500 for western blotting
DNMT3A	Santa Cruz Biotechnology	sc-365769	1:300 for western blotting
DNMT3B	Santa Cruz Biotechnology	sc-376043	1:300 for western blotting
H3K4me3	Abcam	ab8580	ChIP
H3K27me3	Merck Millipore	07-449	ChIP
Alexa Fluor-488 conjugate secondary antibody	Thermo Fisher Scientific		1:500 for immunocytochemistry
Alexa Fluor-546 conjugate secondary antibody	Thermo Fisher Scientific		1:500 for immunocytochemistry
Alexa Fluor-555 conjugate secondary antibody	Thermo Fisher Scientific		1:500 for immunocytochemistry
Goat anti-mouse IgG-HRP	Santa Cruz Biotechnology	sc-2055	1:10000 for western blotting
Goat anti-rabbit IgG-HRP	Agilent	P044801-2	1:10000 for western blotting
Donkey anti-goat IgG-HRP	Santa Cruz Biotechnology	sc-2056	1:10000 for western blotting

HRP, horseradish peroxidase.

Table S3. Microarray analysis of parental and NR5A1-induced cells cultured under TF and CHIR conditions (related to Figure 3)

Comparisons between two samples are as follows,

Comparison 1: Parental-DOX (+) and NR5A1-DOX (+)

Comparison 2: Parental-DOX (+)_CHIR and NR5A1-DOX (+)_CHIR

Comparison 3: NR5A1-DOX (+) and NR5A1-DOX (+)_CHIR

Comparison 4: Parental-DOX (+) and NR5A1-DOX (+)_CHIR

Comparison 5: Parental-DOX (+) and Parental-DOX (+)_CHIR

Table S4. RNA-seq analysis in this study, in human naive-like cell lines (Gafni et al., 2013; Chan et al., 2013; Takashima et al., 2014; Theunissen et al., 2014), and in human embryos (Yan et al., 2013) (related to Figures 3 and 4)

Table S5. RNA-seq analysis of transposable elements (TEs) in parental and NR5A1-induced cells cultured under TF and CHIR conditions (related to Figure 3)

Raw count data obtained from featureCounts and the results of DESeq2 analysis [adjusted p-value < 0.05, $\log_2$ fold change (FC) > 1.5] are shown.

Table S6. RNA-seq analysis of TEs in all samples of this study (related to Figure 4)

Raw count data obtained from featureCounts are shown. The DESeq2 analysis was performed in parental-TF, N1-CHIR, and EOS(N1)-tt2iLGöX cells; false discovery rate (FDR) < 0.05.

Supplemental Experimental Procedures

Plasmid construction

For transcription factor screening, the pLVSIN-EF1α Pur vector was purchased from TaKaRa Bio. After removing the EF1α promoter from the vector, the CAG promoter was inserted to construct the pLVSIN-CAG Pur vector. POU5F1, SOX2, NANOG, and KLF4 cDNAs were obtained from the pDON5 OKSLN vector (TaKaRa Bio) by PCR. The PRDM14 cDNA (Tsuneyoshi et al., 2008) was cloned by PCR, and the cDNAs of TBX3 (IRAL042P10), KLF2 (SC127849), ESRRB (SC327896), NR5A1 (RDB06299), and NR5A2 (RC213887) were purchased from the RIKEN BRC DNA Bank (TBX3 and NR5A1) and OriGENE Technologies (KLF2, ESRRB, and NR5A2). Site-directed mutagenesis of KLF2 and NR5A2 was performed by PCR using primers matching the reference sequences (NP_057354 and NP_003813, respectively).

Cell culture

All hESC lines were used according to the Guidelines on the Distribution and Utilization of Human Embryonic Stem Cells of the Ministry of Education, Culture, Sports, Science, and Technology of Japan. The hESC lines KhES-1 (Kyoto University, Kyoto, Japan) (Suemori et al., 2006) and H9 (WA09; WiCell Research Institute, Madison, WI) (Thomson et al., 1998) and the hiPSC line 253G1 (Kyoto University) (Nakagawa et al., 2008; Takahashi et al., 2007) were maintained on mitomycin-C-treated MEFs in conventional hPSC medium consisting of Dulbecco's modified Eagle's medium (DMEM)/F12 (D6421; Sigma-Aldrich, St. Louis, MO), 20% KSR (Thermo Fisher Scientific, Waltham, MA), 2 mM L-glutamine (G7513; Sigma-Aldrich), 1X non-essential amino acids (M7145; Sigma-Aldrich), 0.1 mM 2-mercaptoethanol, and 5 ng/mL recombinant human FGF2 (Wako, Osaka, Japan).

For feeder-free culture, small clumps of cells were transferred into Matrigel Matrix (growth factor reduced; Corning Inc.)-coated dishes and cultured in mTeSR1 medium (ST-05850; Stemcell Technologies). The dishes were coated with 25 μg/cm^2 Matrigel for at least 1 h at room temperature (RT) before cell seeding. Parental cells were passaged every 3–4 days using 2 mg/mL Dispase (Thermo Fisher Scientific). To culture NR5A transfectants, 0.1 μg/mL DOX (MP Biomedicals) was added, and the medium was changed daily. To select for transgene-expressing cells, puromycin (Sigma-Aldrich) and Zeocin (Thermo Fisher Scientific) were added at 1 and 5 μg/mL, respectively, after at least 5 days of DOX treatment. After cultivation with DOX and antibiotics for 10 days, single cell dissociation was initiated. The cells were incubated with 4 mM ethylenediaminetetraacetic acid (EDTA)/phosphate buffered saline (PBS) for 3–5 min and then with TrypLE Select for 5–10 min at 37°C (the EDTA treatment can be omitted if desired). The dissociated cells were seeded in Matrigel-coated dishes at 1.25–2.5 × 10^4 cells/cm^2 and passaged every 4–5 days.

For cell culture with small molecules, custom mTeSR1 without FGF2 and TGF-β was purchased from Stem Cell Technologies (ST-05896). Note that the previous version of the medium contained three components, LiCl, gamma-aminobutyric acid, and pipecolic acid, but the current version does not. When this study was initiated, only the previous version was available. We have confirmed that the current version is also suitable for this experiment. Small molecules and growth factors were used at the following concentrations, 3 μM CHIR99021 (CHIR; Axon), 1 μM

PD0325901 (PD03; Axon), 2 μM SB431542 (Tocris), 0.25 μM A83-01 (Tocris), and 10 ng/mL recombinant human leukemia inhibitory factor (LIF; Merck Millipore). Induction of naive cells from EOS cells was implemented according to a previously reported chemical resetting protocol (Guo et al., 2017). Briefly, cells cultured on mitomycin-C-treated MEFs were treated with 1 mM valproic acid sodium salt (VPA; Sigma-Aldrich), 1 μM PD03, and 10 ng/mL LIF for the first 3 days in N2B27 medium containing DMEM/F12, Neurobasal (Thermo Fisher Scientific), 0.5× B27 (Thermo Fisher Scientific), 0.5× N2 (Thermo Fisher Scientific), 2 mM L-glutamine, and 0.1 mM 2-mercaptoethanol. The cells were then cultured with 1 μM PD03, 2 μM Gö6983 (Tocris), 2 μM XAV939 (Sigma-Aldrich), and 10 ng/mL LIF for 6 days. For feeder-free culture, single dissociated cells were transferred to tt2iLGö plus XAV939 (tt2iLGöX) medium (0.3 μM CHIR). Geltrex (1 μl/cm^2; Thermo Fisher Scientific) and 10 μM Y-27632 were added to the dishes at each routine passaging. To induce naive cells from EOS-N1 cells, cells cultured under the CHIR condition were transferred to tt2iLGöX medium and cultivated as described above. Experiments were performed in a 5% CO_2 atmosphere under TF and CHIR conditions or in 7% CO_2 and 5% O_2 under the naive condition.

Lentiviral infection

The Lenti-X HTX Packaging System (TaKaRa Bio) was used to transfect pLVSIN-CAG Pur vectors carrying each cDNA, according to manufacturer's instructions. The pMD2.G and psPAX2 vectors were obtained from Addgene (plasmids 12259 and 12260, respectively) to generate vesicular stomatitis virus G-pseudotyped viral particles. Either pLV-tTR-KRAB-IRES-Neo or pLVCT-NR5A-IRES-Puro was co-transfected with pMD2.G and psPAX2 into Lenti-X 293T cells (TaKaRa Bio) using Lipofectamine 2000 Reagent (Thermo Fisher Scientific), according to manufacturers' instructions. The collected virus-containing supernatants were centrifuged and then filtered through a 0.45-μm polyvinylidene fluoride filter (Merck Millipore) to remove cellular debris. The viral stocks were concentrated using a Lenti-X Concentrator (TaKaRa Bio). After centrifugation, the pellets were resuspended in mouse embryonic fibroblast (MEF)-conditioned medium (CM). One day before viral infection, human embryonic stem cells (hESCs) cultured in MEF-CM were dissociated into single cells with TrypLE Select (Thermo Fisher Scientific) and transferred into Matrigel-coated 24-well plates at 5 × 10^4 cells/cm^2 with 10 μM Y-27632 (Wako). The next day, the culture medium was exchanged with the concentrated viral suspension in the presence of 10 μg/mL polybrene. After 24 h of culture, the medium was replaced with fresh MEF-CM, and the cells were maintained on MEFs in CM for human pluripotent stem cell (hPSC) culture. To clone parental cells, tTR-KRAB-Neo-expressing cells were selected on Neo-resistant MEFs with 50 μg/mL G418 (Thermo Fisher Scientific) and seeded at a density of 5,000 cells/60-mm Neo-MEF-containing plate with Y-27632. Formed colonies were isolated and used to examine tet expression by immunocytochemistry.

EOS-GFP transfection

The pPB-EOS-GFP-IP (Plasmid 60439; (Guo et al., 2017; Takashima et al., 2014) and pCMV-hyPBase (Yusa et al., 2011) vectors were obtained from Addgene and the Wellcome Trust Sanger Institute, respectively. Plasmids were transfected into H9 parental cells by electroporation. Puromycin was used to select for GFP-expressing cells at 0.5

μg/mL for EOS and EOS-N1 cells and 1 μg/mL for EOS-reset and EOS(N1) cells.

siRNA transfection

Parental and NR5A1-induced cells were seeded in Matrigel-coated dishes at 5×10^4 and 2.5×10^4 cells/cm^2, respectively. Parental cells were cultured in mTeSR1 in the presence of 10 μM Y-27632 and 0.1 μg/mL DOX. NR5A1-induced cells were cultivated in custom mTeSR1 containing 3 μM CHIR99021 and DOX. Either 10 or 20 nM siRNA was transfected using Lipofectamine RNAiMAX Transfection Reagent (Thermo Fisher Scientific) 24 and 48 h after cell seeding. Cells were treated with lysis buffer ussing a RNeasy Micro Kit (Qiagen) for RNA extraction 24 h after the second transfection. Control (cat. no. 1027286 and 1022076), *DPPA2* (cat. no. SI05171740 and SI04349961), and *DPPA4*, (cat. no. SI00373282 and SI03223024) siRNAs were purchased from Qiagen.

Cell growth rate determination and cell cycle analysis

To analyze the cell growth rate, dissociated cells were seeded on Matrigel-coated 24-well plates at 2.5×10^4 cells/cm^2. Parental cells were cultured in mTeSR1 with 10 μM Y-27632. NR5A1-induced cells were cultured in mTeSR1 or custom mTeSR1 with 2i and LIF in the presence of DOX. Cell viabilities were analyzed every 24 h with acridine orange and propidium iodide staining using a NucleoCounter NC-3000 (ChemoMetec). The doubling time (DT) was calculated according to the American Type Culture Collection Animal Cell Culture Guide (https://www.atcc.org/) using the equation DT = T In2/In (Xe/Xb), where T is the incubation time, Xb is the cell number at the beginning of the incubation time, and Xb is the number at the end of the incubation time. For cell cycle analysis, dissociated cells were seeded onto Matrigel-coated 12-well plates at 2.5×10^4 cells/cm^2 for 24 h. The medium was exchanged with prewarmed fresh medium, and the cells were treated with 10 μM Click-iT EdU (Thermo Fisher Scientific) for 1 h. After labeling, the collected cells were reacted with Alexa Fluor 647 azide and FxCycle Violet Stain (Thermo Fisher Scientific) for flow cytometric analysis. These procedures were performed as described in the instructions for the Click-iT Plus EdU Alexa Fluor 647 Flow Cytometry Kit (Thermo Fisher Scientific).

Teratoma formation assay

Animal experiments were conducted in compliance with the regulations of animal experimentation at Kyoto University with approval by the animal ethics committee. Cells were dissociated by treatment with TrypLE Select and then washed in PBS (-). The collected cell pellets were injected into the testes of 6–8-week-old SCID mice (n = 2 for each cell line). Teratomas were collected 2–3 months after injection. For hematoxylin and eosin staining, the tissues were fixed in Bouin's fixative, embedded in paraffin, and sectioned into 5-μm thick sections. The stained sections were observed using a BZ9000 all-in-one microscope (Keyence). Images were merged using Keyence Analysis Software (Keyence).

Karyotype analysis

Cells were treated with 0.5 μg/mL KaryoMAX Colcemid Solution in PBS (Thermo Fisher Scientific) for 2 h and then

collected by trypsinization. Dissociated cells were incubated in 0.075 M KCl for 12 min at 37°C and then fixed in Carnoy's fixative. After Giemsa staining, at least 30 metaphase spreads were counted.

Oxygen consumption test

Dissociated cells were seeded on a Matrigel-coated 96-well assay plate (Seahorse) at 4×10^4 cells/well 1 day before the assay. Parental cells were cultured in mTeSR1 with 0.1 μg/mL DOX and 10 μM Y-27632. NR5A1-induced cells were cultivated in custom mTeSR1 with DOX and 3 μM CHIR99021. In DOX (–), both parental and NR5A1-induced cells were cultured in mTeSR1 with 10 μM Y-27632. NR5A1-induced cells after withdrawal of DOX were cultured with mTeSR1 with 10 μM Y-27632. An XF Cell Mito Stress Test Kit and XFe96 Analyzer (Seahorse) were used for this experiment. Small molecules were prepared at the following concentrations, 2 μM oligomycin (Abcam), 0.25 μM FCCP (Sigma-Aldrich), 1 μM rotenone (Sigma-Aldrich), and 1 μM antimycin (Sigma-Aldrich) in assay medium consisting of DMEM (D5030; Sigma-Aldrich) with 13.7 mM D-glucose, 0.392 mM sodium pyruvate (Sigma-Aldrich), and 2.94 mM L-glutamine (Sigma-Aldrich). The medium was exchanged with assay medium 1 h before the assay, and the cells were cultured at 37°C at an atmospheric concentration of CO_2. The oxygen consumption rate (OCR) was analyzed using XFe Wave analysis software (Seahorse).

Bisulfite PCR and sequencing

Genomic DNA was extracted using a Gentra Puregene Cell Kit (Qiagen), according to manufacturer's instructions, and 1 μg of DNA was used for bisulfite conversion, followed by PCR amplification. The PCR products were cloned into pGEM®-T easy (Promega). At least 10 clones of each sample were sequenced with T7 universal primer. PCR primer sequences are listed in Table S1. Methylated and unmethylated CpGs were analyzed using the Quantification Tool for Methylation Analysis (Center for Developmental Biology, RIKEN, Japan; http://quma.cdb.riken.jp/index_j.html).

RNA extraction, cDNA synthesis, and real-time PCR analysis

Total RNA was extracted using RNeasy Mini and Micro Kits (Qiagen) according to manufacturer's instructions. Synthesis of cDNA was performed using an Omniscript Reverse Transcription kit (Qiagen) with random primers (TaKaRa Bio). Fast SYBR Green Master Mix (Thermo Fisher Scientific) was used for real-time PCR analysis using a StepOnePlus Real-Time PCR System (Thermo Fisher Scientific). *GAPDH*, *HPRT, ACTB*, and *RPL37A* expression was analyzed using the comparative ΔCt method (Livak and Schmittgen, 2001). Primer sequences used in this study are listed in Table S1.

RNA-fluorescence in situ hybridization (FISH)

RNA-FISH was performed as described previously (Vallot and Rougeulle, 2016). Briefly, cells seeded on Matrigel-coated glass coverslips were incubated in ice-cold CSK buffer (100 mM NaCl, 300 mM sucrose, 3 mM $MgCl_2$, and 10 mM PIPES; pH 6.8) containing 0.5% Triton X-100 and 2 mM Ribonucleoside Vanadyl Complex (VRC;

BioLabs) for 5 min on ice, fixed with 3% paraformaldehyde containing 2 mM VRC for 10 min at RT, and washed three times for 4 min in ice-cold 70% EtOH. After dehydration in 90% and 100% EtOH for 4 min each, the fixed cells were incubated with green 496- (Enzo Life Sciences) or Cy3-labeled (GE Healthcare) probes at 37°C overnight. The next day, the cells were washed twice for 10 min in 50% formamide/2X SSC at 42°C and then washed twice for 5 min in 2X SSC and mounted with Vectashield containing 4,6-diamidino-2-phenylindole (DAPI; Vector Laboratories). Fluorescence was observed under a Zeiss fluorescence microscope (Axio Imager. Z2; Carl Zeiss). The probes were prepared using a Nick Translation Kit (Abbott Molecular) with bacterial artificial chromosome DNAs for *XIST* (CH17-218B21), *XACT* (RP11-35D3), and *HUWE1* (RP11-579N19) obtained from the BACPAC Resources Center. The proportion of cells bearing mono- or bi-allelic expression was determined manually.

Immunocytochemistry

Cells were cultured on dishes for 2–3 days and then fixed in 4% paraformaldehyde for 20 min. After washing with PBS (-), the fixed cells were permeabilized with 0.2% Triton X-100 for 15 min and then blocked with 10% bovine serum albumin and 5% serum in PBS (-) for 30 min. Then, the cells were incubated with primary antibodies for 1 h at RT, following by washing with PBS (-). After incubation with secondary antibodies for 1 h, the washed samples were mounted on glass slides with Vectashield containing DAPI. Fluorescence was observed under the Zeiss fluorescence microscope. Antibodies used in this study are listed in Table S2.

Western blotting

Cells were lysed in radioimmunoprecipitation assay (RIPA) buffer [50 mM Tris-HCl (pH 8.0), 150 mM NaCl, 1% NP40, 0.5% sodium deoxycholate, 0.1% SDS, 2 mM EDTA, and proteinase inhibitor cocktail (PIC; Roche)]. Protein concentrations were determined using a BCA protein assay kit (Thermo Fisher Scientific). Proteins (5–20 μg) were separated by sodium dodecyl sulfate (SDS)-polyacrylamide electrophoresis, then transferred onto polyvinylidene fluoride membranes and incubated in Blocking One (Nacalai Tesque Inc., Kyoto, Japan) at RT for 1 h. Then, the membranes were incubated in Can Get Signal Solution 1 (Toyobo) with primary antibodies at 4°C overnight, following by washing with Tris-buffered saline containing 0.1% Tween 20. Treatment with the secondary antibodies was performed in Can Get Signal Solution 2 (Toyobo) for 1 h at RT. The signals were detected by luminol-based enhanced chemiluminescence (SuperSignal West Dura Extended Duration Substrate; Thermo Fisher Scientific) using a CCD imaging system (LAS3000; FUJIFILM). Antibodies used in this study are listed in Table S2.

Flow cytometric analysis

Expression of pluripotency markers, such as OCT3/4, NANOG, and SOX2, was analyzed using a Human Pluripotent Stem Cell Transcription Factor Analysis Kit (BD Biosciences) and a BD FACS Aria II flow cytometer (BD Biosciences). Percentages of apoptotic populations induced by single cell dissociation were analyzed using an Annexin V Apoptosis Detection Kit I (BD Biosciences). Cell cycle analysis was performed using a Click-iT Plus EdU Alexa

Fluor 647 Flow Cytometry Kit (Thermo Fisher Scientific) and FxCycle Violet Stain. A MACS Quant Analyzer VYB (Miltenyi Biotec) was used for these experiments. All procedures followed the manufacturers' instructions. Flow cytometry data were analyzed using FlowJo software (version 9.9.5; FlowJo LLC).

Microarray data analysis and filter criteria

Total RNA was isolated from tissues using TRIzol Reagent (Invitrogen) and purified using SV Total RNA Isolation System (Promega). cRNA was amplified and labelled using the Low Input Quick Amp Labelling Kit (Agilent Technologies). cRNA was hybridized to a 60K 60-mer oligomicroarray (SurePrint G3 Human Gene Expression Microarray 8x60K v2; Agilent Technologies) according to manufacturer's instructions. Hybridized microarray slides were scanned using an Agilent scanner and the relative hybridization intensities and background hybridization values were calculated using Feature Extraction Software version 9.5.1.1 (Agilent Technologies). Scanned images were analyzed with Feature Extraction Software 9.5.1.1 (Agilent) using default parameters to obtain background subtracted and spatially detrended Processed Signal intensities. Raw signal intensities and flags for each probe were calculated from hybridization intensities (gProcessedSignal) and spot information (gIsSaturated) according to the procedures recommended by Agilent [Flag criteria on GeneSpring Software: Absent (A): "Feature is not positive and significant" and "Feature is not above background". Marginal (M): "Feature is not Uniform", "Feature is Saturated", and "Feature is a population outlier". Present (P): others]. The raw signal intensities of 12 samples were $\log_2$-transformed and normalized by the quantile algorithm using the "preprocessCore" library package (Bolstad et al., 2003) in Bioconductor software (Gentleman et al., 2004). Probes that called the "P" flag in at least one sample were selected, excluding lincRNA probes. We next applied the Linear Models for Microarray Analysis (limma) package (Smyth, 2017) of Bioconductor and obtained 24,169 genes. The criteria were a limma p-value < 0.05 and absolute log-fold-change ($|\log FC| > 1$ (non-log-transformed intensities and ratios are shown in Table S3). Heat maps were generated using MeV software (Saeed et al., 2003) and a principal component analysis (PCA) plot was generated using the ggplot2 package (https://github.com/tidyverse/ggplot2). The hierarchical clustering method was used to sort genes. The color indicates the distance from the median of each row (the distance metric was "Euclidean distance" and the linkage method was "average linkage clustering"). For GO analysis, genes up- or downregulated by > 4-fold were analyzed in the Database of Annotation, Visualization, and Integrated Discovery (DAVID; https://david.ncifcrf.gov/).

RNA extraction, library preparation, and RNA-seq

Total RNA was extracted using TRIzol-LS Reagent (Thermo Fisher Scientific) according to manufacturer's instructions. RNA integrity was evaluated using an Agilent 2100 Bioanalyzer with an Agilent 6000 RNA Pico Kit (Agilent). Libraries for sequencing were prepared using a TruSeq® Stranded mRNA Library Preparation Kit (Illumina) according to manufacturer's instructions. After adapter ligation, purified cDNA was amplified by 15 cycles of PCR. The libraries were evaluated using the Agilent 2100 Bioanalyzer with an Agilent High-Sensitivity DNA Kit (Agilent). Validated libraries were loaded into a MiSeq Reagent Kit v3 (150 cycles) at a final concentration of 10 pM. Sequencing was

performed using a MiSeq sequencer (Illumina) in paired-end mode.

RNA-seq data analysis

RNA-seq data from human naive-like cell lines and embryos were downloaded from the Gene Expression Omnibus (GEO; GSE83765 for 5i/L/A cells, GSE85689 for NHSM cells, GSE123055 for cells in formative transition, and GSE36552 for embryos) and ArrayExpress (E-MTAB-2857 for reset cells and E-MTAB-2031 for 3iL cells). To reduce technical variability in the data, downsampling was performed for datasets with more than 30 million reads (except GSE36552) using the seqtk tool (https://github.com/lh3/seqtk). All RNA-seq datasets included in this study were aligned using STAR (version 2.5.3) to the human genome (UCSC hg19) with 50 bp single-end mode and command options for 2-pass and unique mapping (Dobin et al., 2013). The count data were obtained using htseq-count in HTSeq (version 0.9.1; (Anders and Huber, 2010) with annotation from UCSC hg19. PCA plots were generated by plotPCA (ntop = 500) in the DESeq2 package with the function to calculate variance-stabilizing transformation (Love et al., 2014). For expression analysis, RPKM values were obtained using R (version 3.3.1). Genes were excluded when the sum of the values from all samples was zero (Table S4). Graphical representations were generated by the Integrative Genomics Viewer (Broad Institute) with coverage data normalized to total read counts.

To analyze transposable elements (TEs), RNA-seq datasets were aligned using TopHat (version 2.1.1; (Trapnell et al., 2009) to the human genome (UCSC hg19) with unique mapping and a 76 bp paired-end mode. We used featureCounts in Subread (version 1.5.2(Liao et al., 2014) to calculate read counts on TEs. RepeatMasker annotations were obtained from the University of California Santa Cruz Table Browser. Differentially expressed TEs covered by at least 10 reads between the parental and N1 cell (Table S5) or among parental, N1, and EOS(N1) cells (Table S6) were sorted by the DESeq2 package. The TEs of LTR7-HERVH, LTR5_Hs-HERVK, and SVA elements (adjusted $p < 0.05$, $\log_2$ FC > 1.5 in Fig. 3F, H; FDR < 0.05 in Fig. 4D) are shown in heat maps. All heat maps were generated using the heatmap.2 function of R. Allelic expression of X-linked genes was analyzed in terms of informative SNPs covered by at least 10 reads among the samples used for analysis. Expression of a gene was defined as biallelic when at least 25% of reads from the minor allele were observed, as previously described (Vallot et al., 2017).

ChIP

Parental and NR5A1-induced cells were treated with 4 mM EDTA and TrypLE Select, and then suspended in PBS (-) at 2.5×10^6 cells/mL. For H3K4me3 and H3K27me3 ChIP-seq, the collected cells were crosslinked with 0.5% formaldehyde for 10 min at RT and then quenched with 0.2 M glycine for 5 min. The crosslinked cells were washed with ice-cold PBS (-). To isolate the nuclear fraction, the cell pellet was suspended in ice-cold buffer 1 [0.3 M sucrose, 60 mM KCl, 15 mM NaCl, 5 mM $MgCl_2$, 0.1 mM EDTA, 15 mM Tris-HCl (pH 7.4), 0.5 mM DTT, and 1X PIC (Promega)], and then ice-cold buffer 2 (0.3 M sucrose, 60 mM KCl, 15 mM NaCl, 5 mM $MgCl_2$, 0.1 mM EDTA, 15 mM Tris-HCl pH 7.4, 0.5 mM DTT, and 1X PIC) was added to the cell suspension. After incubation for 10 min on ice, ice-cold buffer 3 (1.2 M sucrose, 60 mM KCl, 15 mM NaCl, 5 mM $MgCl_2$, 0.1 mM EDTA, 15 mM Tris-HCl pH 7.4,

0.5 mM DTT, and 1X PIC) was added, followed by centrifugation at 10,000 × *g* for 30 min at 4°C (himac CP80WX; Hitachi Koki). The collected nuclear extract was suspended in 1X micrococcal nuclease (MNase) digestion buffer (0.32 M sucrose, 50 mM Tris-HCl pH 7.4, 4 mM $MgCl_2$, 1 mM $CaCl_2$, and 1X PIC) and incubated with 75 U (per 1.5×10^7 cells) MNase for 15–20 min at 37°C. EDTA (5 mM) was added to the suspension to stop the reaction. After sonication and centrifugation, the supernatant (Sup 1) was frozen with liquid N_2. The cell pellet was dissolved in dialysis buffer (1 mM Tri-HCl pH. 7.4, 0.2 mM EDTA, and 1X PIC), and the suspension was transferred into a Slide-A-Lyzer Dialysis Cassette (3.5 K MWCO; Thermo Fisher Scientific) and dialyzed against the dialysis buffer overnight. After centrifugation, the supernatant (Sup 2) was frozen in liquid N_2. The pellet was sheared in an S220 Focused-ultrasonicator (Covaris) using the following settings, duty factor: 10%; peak incident power: 175 W; cycles per burst: 200; and time: 180 s. The sheared sample was centrifuged, and the supernatant (Sup 3) was frozen in liquid N_2 until use. For preclearing, a mixture of Sup 1–3 was suspended in ChIP dilution buffer (0.01% SDS, 1% Triton X-100, 1.2 mM EDTA, 16.7 mM Tris-HCl pH 8.1) and 167 mM NaCl) and incubated with Protein A/G PLUS-Agarose Immunoprecipitation Reagent (Santa Cruz Biotechnology) at 4°C for 1 h. After centrifugation, the supernatant was transferred to a new tube. One percent of the input from the supernatant was stored at 4°C. The remainder was incubated with 10 μg antibodies (Table S2) and normal rabbit IgG (Cell Signaling Technology) per 1×10^7 cells at 4°C overnight. Then, Protein A/G PLUS-Agarose was added to the lysate, followed by incubation at 4°C for 4 h. After centrifugation, the pelleted beads were washed once with low salt wash buffer (0.1% SDS, 1% Triton X-100, 2 mM EDTA, 20 mM Tris-HCl pH 8.1, and 150 mM NaCl), once with high salt wash buffer (0.1% SDS, 1% Triton X-100, 2 mM EDTA, 20 mM Tris-HCl pH 8.1, and 500 mM NaCl), once with LiCl wash buffer (0.25 M LiCl, 1% NP-40, 1% sodium deoxycholate, 1 mM EDTA, and 10 mM Tris-HCl pH 8.1), and twice with TE buffer (10 mM Tris-HCl and 1 mM EDTA pH 8.0). The samples and inputs were then eluted with elution buffer (1% SDS and 100 mM $NaHCO_3$). DNA-protein crosslinks were reversed in 250 mM NaCl at 65°C overnight. The samples were then treated with RNase A and proteinase K. DNA was purified by phenol chloroform extraction and ethanol precipitation. The dsDNA was evaluated using an Agilent 2100 Bioanalyzer with the Agilent High-Sensitivity DNA Kit.

For NR5A1 ChIP-seq, the collected cells were crosslinked with 1% formaldehyde for 10 min at RT and quenched with 0.2 M glycine for 5 min. To isolate the nuclear fraction, the crosslinked sample was incubated in lysis buffer 1 (50 mM HEPES-KOH pH 7.5, 140 mM NaCl, 1 mM EDTA, 10% glycerol, 0.5% NP40, 0.25% Triton X-100, and 1X PIC) at 4°C for 10 min and then incubated in lysis buffer 2 (10 mM Tris-HCl pH 8.0, 200 mM NaCl, 1 mM EDTA, 0.5 mM EGTA, and 1X PIC) at 4°C for 10 min. The collected cell pellet was dissolved in lysis buffer 3 (10 mM Tris-HCl pH 8.0, 100 mM NaCl, 1 mM EDTA, 0.5 mM EGTA, 0.1% sodium deoxycholate, 0.5% n-lauroylsarcosine, and 1X PIC) and sheared in the Covaris S220 Focused-ultrasonicator using the following settings, duty factor: 10%; peak incident power: 140 W; cycles per burst: 200; and time: 80 s. For preclearing, the sample was incubated with Protein A/G PLUS-Agarose at 4°C for 1 h. After centrifugation, the supernatant was transferred to a new tube; one percent of the input supernatant was stored at 4°C, while the rest was incubated with 10 μg mouse anti-DDDDK-tag (Table S2) and normal mouse IgG (Santa Cruz Biotechnology) per 1×10^7 cells at 4°C overnight. Subsequent steps

were performed as described above.

Library preparation and ChIP-seq

Libraries for sequencing were prepared using a TruSeq® DNA Sample Preparation Kit (Illumina) according to manufacturer's instructions. After adapter ligation, DNA fragments of 300–400 bp were excised from 2% agarose gels. The purified DNA was amplified by 15–18 cycles of PCR. Libraries were evaluated using an Agilent 2100 Bioanalyzer with the Agilent High-Sensitivity DNA Kit. Validated libraries were loaded into the MiSeq Reagent Kit v3 (150 cycles) at a final concentration of 10 pM. Sequencing was performed in a MiSeq sequencer using the paired-end mode.

ChIP-seq data analysis

All ChIP-seq datasets were aligned to the human genome (UCSC hg19) with up to a single mismatch using Bowtie2 (version 2.2.8; (Langmead et al., 2009). We used the MACS2 (version 2.1.1; (Zhang et al., 2008) peak-finding algorithm to identify regions of ChIP-seq enrichment above the background. Graphical representations were generated using the $\log_{10}$ likelihood ratio. We used ngs.plot (Shen et al., 2014) to construct heat maps and the average profile (avgprof) of the ChIP-seq read density. Heat maps of H3K4me3 and H3K27me3 were prepared spanning the regions ± 5 kb up- and downstream of the TSSs of annotated polycomb-associated genes (3,135 genes; (Theunissen et al., 2014). We also calculated the avgprof of approximately ± 3 kb up- and downstream of polycomb-associated genes for H3K4me3 and H3K27me3. To confirm the bivalent association between H3K4me3 and H3K27me3, we calculated the avgprof of approximately ± 3 kb up- and downstream of peak centers detected by MACS2. To detect H3K4me3 and NR5A1 ChIP signal enrichments on HERVHs, we calculated the avgprof of approximately ± 10 kb up- and downstream of 1,225 HERVH regions (Wang et al., 2014). MEME-ChIP was used to search for the motif (Bailey et al., 2009).

Statistical analysis

Error bars in figures represent the standard deviation (s.d.) or standard error of the mean (s.e.m) of three biological replicates, unless otherwise indicated. Statistical significance was determined using the two-tailed unpaired Student's *t*-test for two group comparisons. Multiple group comparisons were performed using one-way analysis of variance with Dunnett's multiple comparison test. P values < 0.05 were considered statistically significant. No samples were excluded from the analyses, and no blinding or randomization was performed in this study.

Supplemental References

Anders, S., and Huber, W. (2010). Differential expression analysis for sequence count data. Genome Biol. *11*, R106.

Bailey, T.L., Boden, M., Buske, F.A., Frith, M., Grant, C.E., Clementi, L., Ren, J., Li, W.W., and Noble, W.S. (2009). MEME SUITE: tools for motif discovery and searching. Nucleic Acids Res. *37*, W202–208.

Bolstad, B.M., Irizarry, R.A., Astrand, M., and Speed, T.P. (2003). A comparison of normalization methods for high density oligonucleotide array data based on variance and bias. Bioinformatics *19*, 185–193.

Dobin, A., Davis, C.A., Schlesinger, F., Drenkow, J., Zaleski, C., Jha, S., Batut, P., Chaisson, M., and Gingeras, T.R. (2013). STAR: ultrafast universal RNA-seq aligner. Bioinformatics *29*, 15–21.

Gentleman, R.C., Carey, V.J., Bates, D.M., Bolstad, B., Dettling, M., Dudoit, S., Ellis, B., Gautier, L., Ge, Y., Gentry, J.*, et al.* (2004). Bioconductor: open software development for computational biology and bioinformatics. Genome Biol. *5*, R80.

Guo, G., von Meyenn, F., Rostovskaya, M., Clarke, J., Dietmann, S., Baker, D., Sahakyan, A., Myers, S., Bertone, P., Reik, W.*, et al.* (2017). Epigenetic resetting of human pluripotency. Development *144*, 2748–2763.

Kim, K.P., Thurston, A., Mummery, C., Ward-van Oostwaard, D., Priddle, H., Allegrucci, C., Denning, C., and Young, L. (2007). Gene-specific vulnerability to imprinting variability in human embryonic stem cell lines. Genome Res. *17*, 1731–1742.

Langmead, B., Trapnell, C., Pop, M., and Salzberg, S.L. (2009). Ultrafast and memory-efficient alignment of short DNA sequences to the human genome. Genome Biol. *10*, R25.

Liao, Y., Smyth, G.K., and Shi, W. (2014). featureCounts: an efficient general purpose program for assigning sequence reads to genomic features. Bioinformatics *30*, 923–930.

Livak, K.J., and Schmittgen, T.D. (2001). Analysis of relative gene expression data using real-time quantitative PCR and the 2(-Delta Delta C(T)) method. Methods *25*, 402–408.

Love, M.I., Huber, W., and Anders, S. (2014). Moderated estimation of fold change and dispersion for RNA-seq data with DESeq2. Genome Biol. *15*, 550.

Nakagawa, M., Koyanagi, M., Tanabe, K., Takahashi, K., Ichisaka, T., Aoi, T., Okita, K., Mochiduki, Y., Takizawa, N., and Yamanaka, S. (2008). Generation of induced pluripotent stem cells without Myc from mouse and human fibroblasts. Nat. Biotechnol. *26*, 101–106.

Rostovskaya, M., Stirparo, G.G., and Smith, A. (2019). Capacitation of human naive pluripotent stem cells for multi-lineage differentiation. Development *146*.

Saeed, A.I., Sharov, V., White, J., Li, J., Liang, W., Bhagabati, N., Braisted, J., Klapa, M., Currier, T., Thiagarajan, M.*, et al.* (2003). TM4: a free, open-source system for microarray data management and analysis. Biotechniques *34*, 374–378.

Shen, L., Shao, N., Liu, X., and Nestler, E. (2014). ngs.plot: Quick mining and visualization of next-generation sequencing data by integrating genomic databases. BMC Genomics *15*, 284.

Smyth, G.K. (2017). Bioinformatics and Computational Biology Solutions Using R | Robert Gentleman | Springer.

Suemori, H., Yasuchika, K., Hasegawa, K., Fujioka, T., Tsuneyoshi, N., and Nakatsuji, N. (2006). Efficient establishment of human embryonic stem cell lines and long-term maintenance with stable karyotype by enzymatic bulk passage. Biochem. Biophys. Res. Commun. *345*, 926–932.

Takahashi, K., Tanabe, K., Ohnuki, M., Narita, M., Ichisaka, T., Tomoda, K., and Yamanaka, S. (2007). Induction of pluripotent stem cells from adult human fibroblasts by defined factors. Cell *131*, 861–872.

Takashima, Y., Guo, G., Loos, R., Nichols, J., Ficz, G., Krueger, F., Oxley, D., Santos, F., Clarke, J., Mansfield, W.*, et*

al. (2014). Resetting Transcription Factor Control Circuitry toward Ground-State Pluripotency in Human. Cell *158*, 1254–1269.

Theunissen, T.W., Powell, B.E., Wang, H., Mitalipova, M., Faddah, D.A., Reddy, J., Fan, Z.P., Maetzel, D., Ganz, K., Shi, L.*, et al.* (2014). Systematic identification of culture conditions for induction and maintenance of naive human pluripotency. Cell Stem Cell *15*, 471–487.

Thomson, J.A., Itskovitz-Eldor, J., Shapiro, S.S., Waknitz, M.A., Swiergiel, J.J., Marshall, V.S., and Jones, J.M. (1998). Embryonic stem cell lines derived from human blastocysts. Science *282*, 1145–1147.

Trapnell, C., Pachter, L., and Salzberg, S.L. (2009). TopHat: discovering splice junctions with RNA-Seq. Bioinformatics *25*, 1105–1111.

Tsuneyoshi, N., Sumi, T., Onda, H., Nojima, H., Nakatsuji, N., and Suemori, H. (2008). PRDM14 suppresses expression of differentiation marker genes in human embryonic stem cells. Biochem. Biophys. Res. Commun. *367*, 899–905.

Vallot, C., Patrat, C., Collier, A.J., Huret, C., Casanova, M., Liyakat Ali, T.M., Tosolini, M., Frydman, N., Heard, E., Rugg-Gunn, P.J.*, et al.* (2017). XACT Noncoding RNA Competes with XIST in the Control of X Chromosome Activity during Human Early Development. Cell Stem Cell *20*, 102–111.

Vallot, C., and Rougeulle, C. (2016). Single-cell Visualization of Chromosome Transcriptional Territories by RNA-paint. Bio. Protoc. *6*.

Wang, J., Xie, G., Singh, M., Ghanbarian, A.T., Rasko, T., Szvetnik, A., Cai, H., Besser, D., Prigione, A., Fuchs, N.V.*, et al.* (2014). Primate-specific endogenous retrovirus-driven transcription defines naive-like stem cells. Nature *516*, 405–409.

Yusa, K., Zhou, L., Li, M.A., Bradley, A., and Craig, N.L. (2011). A hyperactive piggyBac transposase for mammalian applications. Proc. Natl. Acad. Sci. U S A *108*, 1531–1536.

Zhang, Y., Liu, T., Meyer, C.A., Eeckhoute, J., Johnson, D.S., Bernstein, B.E., Nusbaum, C., Myers, R.M., Brown, M., Li, W.*, et al.* (2008). Model-based analysis of ChIP-Seq (MACS). Genome Biol. *9*, R137.